Journal of Molecular and Cellular Cardiology 112 (2017) 83–90

Contents lists available at ScienceDirect

Journal of Molecular and Cellular Cardiology

journal homepage: www.elsevier.com/locate/yjmcc

Heterozygous deletion of AKT1 rescues cardiac contractility, but not hypertrophy, in a mouse model of Noonan Syndrome with Multiple Lentigines

Rajika Roy, Maike Krenz*

Dalton Cardiovascular Research Center, Department of Medical Pharmacology & Physiology, School of Medicine, University of Missouri, 134 Research Park Dr, Columbia, MO 65211, United States

ARTICLE INFO

Keywords:
SHP2
AKT
Cardiac hypertrophy
Cardiomyopathy
Phosphatase
Signal transduction

ABSTRACT

Noonan Syndrome with Multiple Lentigines (NSML) is associated with congenital heart disease in form of pulmonary valve stenosis and hypertrophic cardiomyopathy (HCM). Genetically, NSML is primarily caused by mutations in the non-receptor protein tyrosine phosphatase SHP2. Importantly, certain SHP2 mutations such as Q510E can cause a particularly severe form of HCM with heart failure in infancy. Due to lack of insight into the underlying pathomechanisms, an effective custom-tailored therapy to prevent heart failure in these patients has not yet been found.

SHP2 regulates numerous signaling cascades governing cell growth, differentiation, and survival. Experimental models have shown that NSML mutations in SHP2 cause dysregulation of downstream signaling, in particular involving the protein kinase AKT. AKT, and especially the isoform AKT1, has been shown to be a major regulator of cardiac hypertrophy. We therefore hypothesized that hyperactivation of AKT1 is required for the development of Q510E-SHP2-induced HCM. We previously generated a transgenic mouse model of NSML-associated HCM induced by Q510E-SHP2 expression in cardiomyocytes starting before birth. Mice display neonatal-onset HCM with initially preserved contractile function followed by functional decline around 2 months of age. As a proof-of-principle study, our current goal was to establish to which extent a genetic reduction in AKT1 rescues the Q510E-SHP2-induced cardiac phenotype in vivo. AKT1 deletion mice were crossed with Q510E-SHP2 transgenic mice and the resulting compound mutant offspring analyzed. Homozygous deletion of AKT1 greatly reduced viability in our NSML mouse model, whereas heterozygous deletion of AKT1 in combination with Q510E-SHP2 expression was well tolerated. Despite normalization of pro-hypertrophic signaling downstream of AKT, heterozygous deletion of AKT1 did not ameliorate cardiac hypertrophy induced by Q510E-SHP2. However, the functional decline caused by Q510E-SHP2 expression was effectively prevented by reducing AKT1 protein. This demonstrates that AKT1 plays an important role in the underlying pathomechanism. Furthermore, the functional rescue was associated with an increase in the capillary-to-cardiomyocyte ratio and normalization of capillary density per tissue area in the compound mutant offspring. We therefore speculate that limited oxygen supply to the hypertrophied cardiomyocytes may contribute to the functional decline observed in our mouse model of NSML-associated HCM.

1. Introduction

In most cases of non-syndromic hypertrophic cardiomyopathy (HCM), systolic contractile performance of the left ventricle (LV) is normal or even elevated. Only a small subset of patients with 'classic' forms of HCM develop systolic heart failure in end-stage disease [1,2]. Therefore, treatment strategies for patients with HCM are mostly focused on reducing the risks of arrhythmias and sudden death as well as ameliorating symptoms caused by outflow tract obstruction and diastolic dysfunction [3]. In contrast, HCM associated with Noonan Syndrome with Multiple Lentigines (NSML, formerly termed LEOPARD Syndrome) can lead to serious contractile dysfunction in children. In

Abbreviations: +, transgenic; AKT, protein kinase B; HCM, hypertrophic cardiomyopathy; LV, left ventricle; LVAWd, LV anterior wall thickness at end-diastole; LVIDd, LV inner diameter at end-diastole; LVPWd, LV posterior wall thickness at end-diastole; MHC, myosin heavy chain; mTOR, mechanistic target of rapamycin; NTG, nontransgenic; NSML, Noonan Syndrome with Multiple Lentigines; PHLPP1, PH domain and leucine rich repeat protein phosphatase 1; WGA, wheat germ agglutinin

* Corresponding author.
E-mail address: krenzm@missouri.edu (M. Krenz).

http://dx.doi.org/10.1016/j.yjmcc.2017.09.003
Received 5 July 2017; Received in revised form 24 August 2017; Accepted 10 September 2017
Available online 11 September 2017

particular, the Q510E mutation in the protein tyrosine phosphatase SHP2 (encoded by *PTPN11*) results in a severe biventricular form of HCM and heart failure already in infancy [4–7]. Mortality is very high and heart transplantation is often the only option to improve survival for patients carrying the Q510E-SHP2 mutation.

The reasons why these forms of HCM lead to heart failure are still unknown. Genetically, most non-syndromic forms of HCM are caused by mutations in various sarcomeric proteins [8], whereas mutations in the signaling regulator SHP2 are responsible for the majority of NSML-associated HCM cases. Recent in vitro studies have shown that NSML mutations in SHP2 result in increased activation of focal adhesion kinase, phosphatidylinositol-3-kinase, protein kinase B (AKT) and mechanistic target of rapamycin (mTOR) [9–11]. Supporting a central role of the latter signaling mediator in the pathomechanism of NSML-associated HCM, mouse models of NSML have revealed that inhibition of mTOR with rapamycin can ameliorate cardiomyocyte hypertrophy [12,13]. However, rapamycin failed to rescue the functional decline caused by Q510E-SHP2 expression in the mouse heart [13], suggesting that pharmacological intervention targeted at mTOR may have been too far downstream to completely rescue the phenotype. One step further upstream, AKT controls mTOR activity via tuberous sclerosis factor 2 and Rheb [14,15]. Interestingly, it has been demonstrated that inhibition of mTOR can result in suppression of a negative feedback loop that in turn increases the activity of AKT and other kinases [16]. Consequently, inhibition of AKT instead of mTOR may be more effective as a treatment for HCM induced by Q510E-SHP2 expression.

AKT (and in particular the AKT1 isoform) has been shown to play a critical role in the regulation of cardiac hypertrophy [17]. However, AKT's role in NSML-associated HCM may not be straightforward. Prior studies have provided strong evidence that moderate increases in AKT activity do not result in pathologic alterations in the heart and even have cardioprotective effects. For example, physiological stress such as exercise has been shown to increase AKT activation in normal mice [18]. In addition, deletion of PH domain and leucine rich repeat protein phosphatase 1 (PHLPP1) increased AKT activity without affecting cardiomyocyte size or contractility and was beneficial under pathological stress in form of chronic pressure overload [19]. Furthermore, nuclear targeting of AKT also did not induce cardiac hypertrophy, and induced protective effects after pressure overload [20,21]. Importantly, only prolonged transgenic activation of AKT at high levels led to ventricular dilation and death [22]. These findings would argue against the increase in AKT activity observed in NSML models playing a causal role in the HCM pathomechanism. On the other hand, we recently found that pharmacological AKT inhibition prevents cardiomyocyte hypertrophy induced by Q510E-SHP2 expression in culture [11], which supports the notion that AKT promotes pathologic cardiac hypertrophy in NSML.

To resolve this controversy and evaluate AKT1 as a potential new therapeutic target, the goal of our current study was to examine the role of AKT1 in NSML by conducting a genetic rescue experiment. Based on our prior data, we hypothesized that increased signaling through AKT1 is necessary for the development of cardiac hypertrophy and contractile dysfunction in the context of NSML. To test our hypothesis, we crossed Q510E-SHP2 transgenic mice with AKT1 deletion mice [23] and characterized the phenotype of the compound mutant offspring. Importantly, deletion of one AKT1 allele by itself does not result in overt cardiac pathology in adult mice and does not alter susceptibility to stressors such as transverse aortic banding [24]. Therefore, this approach is well suited for proof-of-principle studies to determine whether AKT1 plays an important role in the pathomechanism of NSML-associated HCM.

2. Methods

2.1. Animals

All animal studies were conducted in accordance with the Institute of Laboratory Animal Research Guide for the Care and Use of Laboratory Animals. All procedures were submitted to and approved by the Animal Care and Use Committee of the University of Missouri. Transgenic mice expressing Q510E-SHP2 driven by the β-MHC promoter were previously generated and described [13,25]. Only the lowest-expressing transgenic line (2.7-fold over endogenous SHP2 levels) was used and crossed from FVB/N into the C57BL/6J strain background for over 14 generations. Subsequently, Q501E-SHP2 transgenic mice were crossed with AKT1 deletion mice (B6.129P2-Akt1^{tm1Mbb}/J, JAX stock number 004912) [23].

2.2. Gravimetry, tissue harvest

All tissue harvests were performed under deep isoflurane inhalation anesthesia. For protein analyses, hearts were rinsed in cold phosphate-buffered saline before weighing and freezing in liquid nitrogen. To arrest hearts in end-diastole for histological studies, hearts were perfused under deep isoflurane anesthesia through the apex with 4% paraformaldehyde in phosphate-buffered saline containing 25 mM KCl and 5% dextrose (cardioplegic buffer).

2.3. Western blotting

Flash-frozen LV tissues were homogenized in lysis buffer (150 mM NaCl, 10 mM Tris, pH 7.4, 1% Triton-X, 1 × Halt Protease & Phosphatase Inhibitor Cocktail (Sigma-Aldrich)). Proteins were separated by SDS-PAGE and transferred to polyvinylidene difluoride membranes (Bio-Rad). For Western blotting, we used anti-SHP2 (SH-PTP2, C-18, rabbit polyclonal, catalog number sc-280, Santa Cruz Biotechnology), anti-phospho-AKT (pS472/pS473, 104A282, mouse monoclonal, catalog number 550747, BD Pharmingen) and the following antibodies obtained from Cell Signaling Technologies: AKT1 (C73H10, rabbit monoclonal, catalog number 2938), GAPDH (D16H11, rabbit monoclonal, catalog number 5174), S6 (54D2, mouse monoclonal, catalog number 2317), and phospho-S6 (S240/244, D68F8, rabbit monoclonal, catalog number 5364). All phospho-specific antibodies were used at 1:500 dilution, all other antibodies at 1:1000. Phosphorylated and total protein bands were quantified using the Bio-Rad ChemDoc imaging system (Bio-Rad). For densitometry (Bio-Rad Quantity One and Image Lab software), rectangular regions of interest of identical size and shape in each lane were drawn tightly around the respective bands. Background signal intensities were determined by placing rectangular regions of interest of identical size and shape in adjacent empty areas in each individual lane. Background intensities were substracted from the respective band intensities measured. Non-specific bands were not included in any of the regions of interest. For all membranes, band intensities were normalized to the GAPDH signal obtained on the same membrane. In addition, Ponceau staining (Sigma-Aldrich) was used to confirm that there were no changes in GAPDH expression compared to total protein loading.

2.4. Echocardiography

Echocardiograms were performed under inhalation anesthesia (1.2–1.8% isoflurane, 0.6 L flow of O_2) using either a GE Vivid-i ultrasound system (GE Healthcare) with a 12 MHz transducer or a Vevo 2100 ultrasound system (Visualsonics) with a 40 MHz transducer. Anesthetized animals were kept warm in supine position for 25 min to ensure hemodynamic stability before image acquisition was started. No data were excluded except for rare cases where hemodynamic instability was evident (such as non-uniform ventricular performance in consecutive beats, heart rate instability, or LV dilation to > 4 mm end-diastolic diameter). M-mode echocardiography was performed using the parasternal short-axis view of the LV. The guidelines of the American Society of Echocardiography were used for measurement of the LV end-diastolic and end-systolic diameters, and anterior and posterior wall thickness. Images were captured digitally and 6 consecutive cardiac cycles were measured and averaged for each animal.

Fig. 1. Mendelian ratios of genotype combinations and heart morphology in offspring from β-MHC-Q510E-SHP2 × AKT1 deletion crosses. A) Genotypes of 240 pups from 37 litters resulting from +;WT/WT × NTG;WT/− matings were determined at two weeks of age. Genotypes were distributed according to expected Mendelian ratios. B) Genotypes of 266 pups from 59 litters resulting from +;WT/− × NTG;WT/− matings were determined at two weeks of age. +;−/− offspring were greatly underrepresented, the expected frequency would have been 12.5%. C) Images of hearts excised from 10 month-old male mice (all from the same litter). All scale bars, 2 mm.

2.5. Immunohistochemistry

Hearts fixed in cardioplegic buffer were embedded in Tissue-TEK O.C.T. compound (Electron Microscopy Sciences), frozen, and sectioned at 5 μm thickness. Sections were obtained exactly in the middle of the heart where the right and left ventricular cavity areas were largest and leaflets of both mitral and tricuspid valves were seen in the same plane. Sections were stained with fluorescently labeled WGA (Invitrogen) and fluorescently labeled isolectin IB_4 (Invitrogen). Random areas of the LV free wall and septum were photographed at 100 × magnification using an IX51 microscope (Olympus). Capillary numbers per area and cross-sectional cardiomyocyte areas were quantified by a blinded investigator using Image J software.

2.6. Statistics

No data were excluded with the exception of echocardiography recordings from hemodynamically unstable mice as described above. All graphs show individual data points as well as mean +/− SEM and p values for all pertinent comparisons unless $p \geq 0.1$. $p < 0.05$ was considered significant. Multiple groups were compared using two-way analysis of variance (ANOVA) followed by post-hoc tests (Holm-Šidák method) using SigmaPlot software. Unpaired Student t-tests were used to compare SHP2 and AKT1 protein expression data from the respective two groups (Fig. 3A,B).

3. Results

We recently generated a transgenic mouse model of NSML-associated HCM in the FVB/N strain background by introducing a β-myosin heavy chain (MHC) promoter cassette containing Q510E-SHP2 cDNA. Detailed phenotype analyses revealed that these mice develop neonatal-onset HCM [13]. To summarize, the mice exhibit increased cardiomyocyte cross-sectional areas, heart-to-body weight ratios, interventricular septum thickness, and cardiomyocyte disarray already as newborns. In adult mice, interstitial fibrosis can be detected and contractile function is depressed. Valve disease is not evident in this mouse model. Since we took a transgenic approach, potential gene dosage effects were carefully excluded by generating a separate mouse model overexpressing wild-type SHP2 protein driven by the β-MHC promoter [26]. For the current study, the transgenic mice expressing Q510E-SHP2 driven by the β-MHC promoter were crossed from FVB/N into the C57BL/6J strain for over 14 generations. Importantly, the change in genetic background did not alter the HCM phenotype in terms of degree of hypertrophy, contractile dysfunction, cardiomyocyte disarray, etc.

In the following, all figures include data from normal littermate controls as well as from transgenic mice with cardiac-specific expression of Q510E-SHP2 and normal AKT1 levels demonstrating the baseline HCM phenotype. Throughout the manuscript, genotypes are indicated as follows: nontransgenic (NTG) or transgenic (+) for β-MHC-Q510E SHP2; two wild type alleles of AKT1 (WT/WT), one wild type and one deleted allele of AKT1 (WT/−), or deletion of both alleles of AKT1 (−/−).

3.1. Breeding strategy and Mendelian ratios

First, +;WT/WT mice were mated with NTG;WT/− mice, yielding +;WT/− offspring at expected Mendelian ratios (Fig. 1A). We noted average litter sizes of 6.5 pups, which is within the normal range for the C57BL/6J substrain. Subsequently, +;WT/− mice were mated with NTG;WT/− mice. In these crosses, average litter size was only 4.5 pups when counted at two weeks of age, suggesting lethality of certain genotype combinations. Genotyping of all live pups at two weeks of age revealed that only 1% of the surviving offspring were +;−/− (Fig. 1B), indicating nearly complete lethality of the combination of the β-MHC-Q510E SHP2 transgene with complete deletion of AKT1. Most likely, the +;−/− genotype was lethal around or early after birth as exploratory timed pregnancies showed that +;−/− pups were alive at embryonic day 17.5 (data not shown). Therefore, we did not continue the +;WT/− × NTG;WT/− matings and focused only on generating +;WT/− mice together with their respective littermate controls by mating +;WT/WT × NTG;WT/−. Animals were aged up to 12 months and neither +;WT/WT nor +;WT/− animals demonstrated increased mortality in this time frame. We did not note any obvious gender effects in the resulting offspring. To allow for direct comparison with our prior study testing the efficacy of rapamycin [13], we focused on data from male offspring in this manuscript.

3.2. Heart morphology and gravimetry

Fig. 1 shows representative images of adult littermate hearts excised at 10 months of age. Expression of Q510E-SHP2 increased heart size (NTG;WT/WT compared to +;WT/WT in Fig. 1C). Deletion of one AKT1 allele reduced heart size slightly. However, the +;WT/− heart still appeared larger than the NTG;WT/− heart, suggesting that the reduction in AKT1 expression may not have reversed the pro-hypertrophic effects of Q510E-SHP2 expression. For exact quantification of hypertrophy, heart weights as well as body weights and tibia lengths were determined in 45 mice at 5 and 28 mice at 10 months of age (Fig. 2). Both data sets were consistent, indicating that the degree of hypertrophy and differences between groups were not dependent on age. Heart weights were increased by the expression of Q501E-SHP2 regardless of whether only one or both alleles of AKT1 were present (Fig. 2A,A′). Body weight was mildly decreased by Q501E-SHP2 expression in young adult mice (Fig. 2B), but in older mice these trends did not reach statistical significance (Fig. 2B′). There were no significant differences in tibia length between groups (data not shown). Heart-to-body weight ratios (Fig. 2C,C′) as well as heart weight-to-tibia length ratios (Fig. 2D,D′) were significantly increased by Q501E-SHP2 expression regardless of age. Importantly, heart-to-body weight and

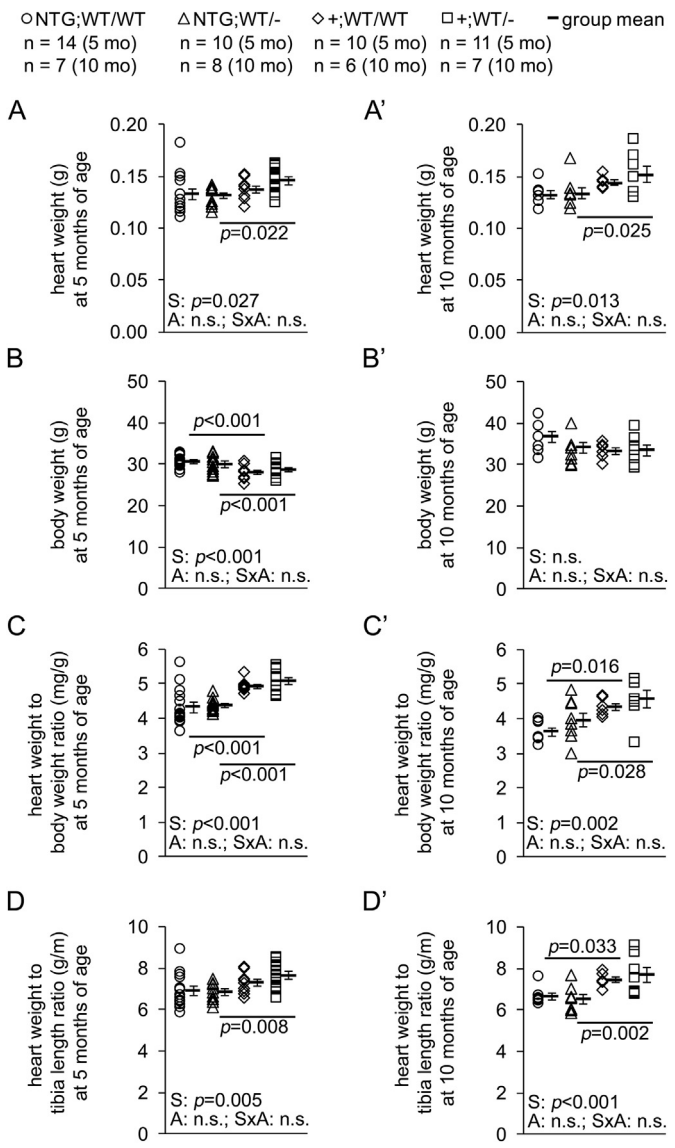

Fig. 2. Gravimetric data. In all panels, individual data and group means +/− SEM are shown. Sample sizes for all groups are listed at the top. For all variables, graphs in the left column summarize data from 5 month-old mice, and graphs on the right show data from 10 month-old mice. S, genotype regarding presence or absence of the Q510E-SHP2 transgene; A, genotype regarding presence of one or two AKT1 alleles; S × A, interaction between S and A. A,A′) Heart weights (including both ventricles and atria) were increased by Q510E-SHP2 expression. B,B′) Body weights were decreased by Q510E-SHP2 expression only in 5 but not in 10 month-old mice. C,C′) Heart-to-body weight ratios were increased by Q510E-SHP2 expression regardless of the level of AKT1 expression. D,D′) Heart weight-to-tibia length ratios were increased by Q510E-SHP2 expression regardless of the level of AKT1 expression.

heart weight-to-tibia length ratios were not normalized by a reduction in AKT1 expression. This indicates that the degree of hypertrophy in our NSML model was not rescued by the deletion of one allele of AKT1.

3.3. Western blotting

Before conducting more detailed in vivo analyses of the HCM phenotype in the crossed mice, we ascertained that deletion of one AKT1 allele in hearts expressing Q510E-SHP2 indeed led to normalization of signaling through this pathway as expected. First, we confirmed the level of SHP2 expression in our NSML model using Western blotting. Similar to our prior findings in the FVB/N background, Q510E-SHP2 was overexpressed in C57BL/6J transgenic mice 2.7-fold over endogenous levels (Fig. 3A,A′). Next, we confirmed that deletion of one AKT1 allele reduced total AKT1 protein content in the respective groups as expected (Fig. 3B,B′). We also probed for phospho-AKT1 to assess relative phosphorylation levels at amino acid S473. Deletion of one AKT1 allele resulted in a compensatory 3-fold increase in relative phosphorylation of the remaining AKT1 protein, regardless of the presence or absence of Q510E-SHP2 expression. These Western blots also showed that the ratio of phospho-AKT1/AKT1 was only slightly increased in +;WT/WT mice compared to NTG;WT/WT controls without reaching statistical significance (Fig. 3C). Using antibodies that were not specific for individual AKT isoforms, we previously observed a significant increase in phospho-AKT/AKT in FVB/N mice [13], so either the change in genetic background or differences in phosphorylation status of AKT2 or AKT3 could explain these different findings. Since the amino acid sequences around the phosphorylation sites are very similar among the three AKT isoforms, additional isoform-specific phospho-antibodies were unlikely to completely resolve this issue. Therefore, relative phosphorylation of S6 was quantified to obtain a downstream readout of AKT pathway activation (Fig. 3D,D′,E′). The ratio of phospho-S6/S6 was similar in NTG;WT/− compared to NTG;WT/WT mice, indicating that the compensatory increase in phospho-AKT1/AKT1 we had observed resulted in normal levels of downstream signaling. Due to high variability, the increase in phospho-S6/S6 in +;WT/WT compared to NTG;WT/WT narrowly missed statistical significance (Fig. 3D). Importantly, the ratio of phospho-S6/S6 in the +;WT/− group was significantly reduced compared to the respective levels in +;WT/WT heart tissue samples. This indicates that deletion of one AKT1 allele effectively reduced the level of S6 activation in hearts expressing Q510E-SHP2 as we had expected.

3.4. Echocardiography

For a more detailed assessment of in vivo cardiac morphology and function, echocardiography was performed. Data from 5 month-old mice were obtained using a pediatric echocardiography system with a 12 MHz probe, whereas 10 month-old mice were imaged with a high-resolution ultrasound system at 30–40 MHz. The two data sets are presented separately (Fig. 4), and the findings are highly consistent. In terms of contractile performance, both fractional shortening and ejection fraction were significantly depressed in mice expressing Q510E-SHP2 with normal levels of AKT1 (Fig. 4A,A′,B,B′). Importantly, deletion of one AKT1 allele normalized both fractional shortening and ejection fraction at 5 and 10 months of age. However, the functional improvement was not accompanied by a rescue of the degree of hypertrophy. Q510E-SHP2 expression increased end-diastolic thickness of the anterior and posterior walls of the LV independent of the level of AKT1 expression. This was consistent in both age groups (Fig. 4 C,D and C′,D′). In line with the definition of concentric hypertrophy, LV inner diameter at end-diastole was reduced by Q510E-SHP2 expression. Comparing the data from the NTG;WT/− to the +;WT/− group, this effect reached statistical significance in both age groups (Fig. 4E,E′).

3.5. Histology

As the Q510E-SHP2 mouse model of NSML-associated HCM exhibits only very mild levels of interstitial fibrosis with isolated foci, we did not quantify the extent of fibrosis in detail in this study. To determine cardiomyocytes size, cryosections through the center of the LV from 10 month-old hearts were stained with fluorescent wheat germ agglutinin (WGA) conjugates to outline sarcolemmal membranes. In parallel, fluorescently labeled isolectin was used to visualize capillaries. Cross-sectional cardiomyocyte areas were significantly increased by Q510E-SHP2 expression. Reducing the level of AKT1 protein by itself had no effect on cardiomyocyte cross-sectional areas. Furthermore, loss of one AKT1 allele did not normalize cross-sectional areas of cardiomyocytes expressing Q51E-SHP2 (Fig. 5A). Due to the increase in size, the number of cardiomyoyctes counted per area was decreased in sections

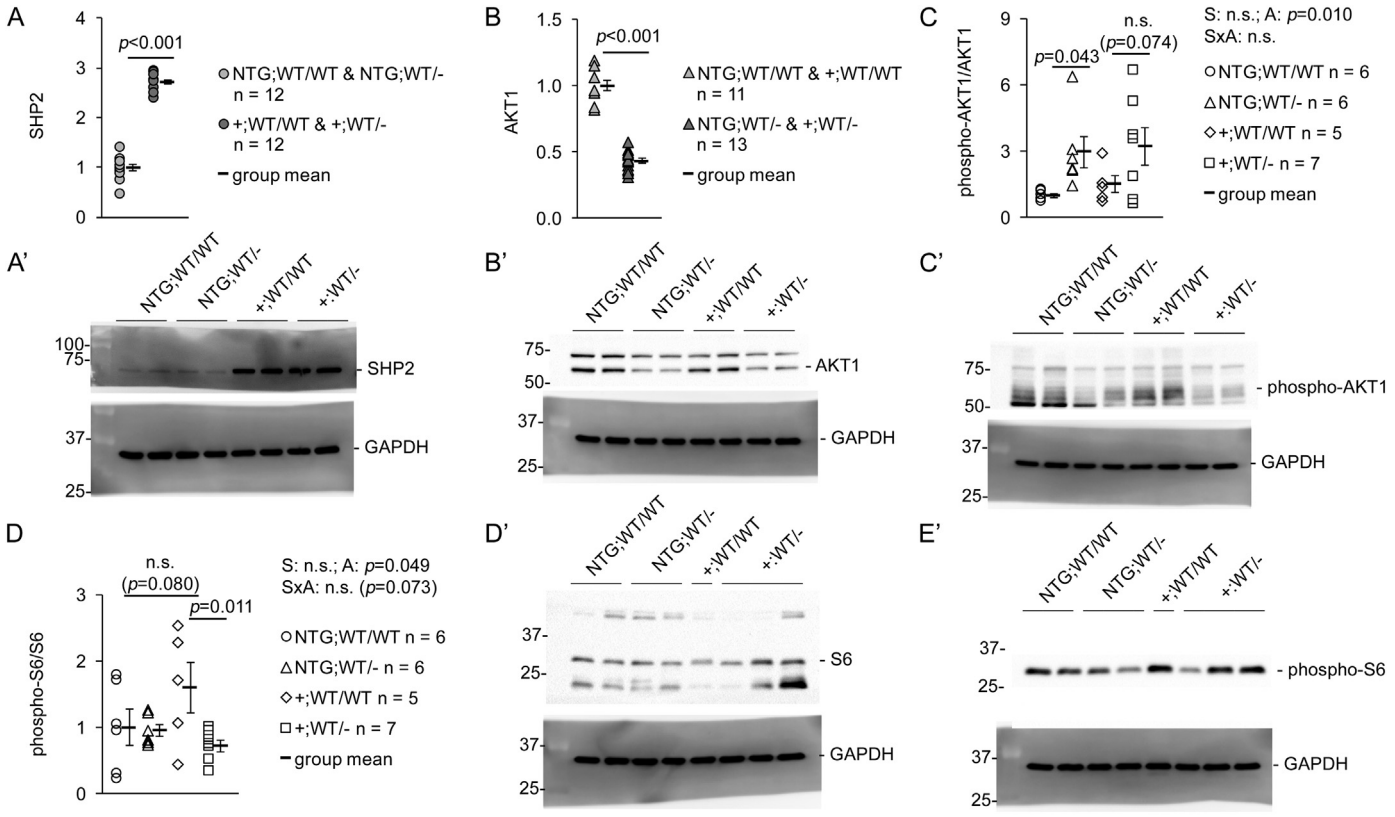

Fig. 3. Western blots for SHP2/AKT1 total protein expression and AKT1/S6 phosphorylation status. In all graphs, individual data and group means +/− SEM are shown. Sample sizes for all groups are listed in the respective legends. Image panels show representative Western blots. All membranes were also probed for GAPDH as a loading control (shown directly underneath for each instance). S, genotype regarding presence or absence of the Q510E-SHP2 transgene; A, genotype regarding presence of one or two AKT1 alleles; S × A, interaction between S and A. A,A′) Transgenic expression of Q510E-SHP2 increased total SHP2 protein levels 2.7-fold over endogenous levels. B,B′) Deletion of one AKT1 allele resulted in decrease of AKT1 protein to 43% of normal levels. C,C′) Deletion of one AKT1 allele caused a 3-fold increase in the relative phosphorylation level of the remaining AKT1 protein. Q510E expression only led to a minor (50% without reaching statistical significance) increase in relative AKT1 phosphorylation. D,D′,E′) Q510E expression only led to a minor (60% without reaching statistical significance) increase in relative S6 phosphorylation. If Q510E expression was combined with heterozygous AKT1 deletion, relative S6 phosphorylation levels were significantly reduced to control levels.

from hearts expressing Q510E-SHP2 regardless of AKT1 levels (Fig. 5B). These findings are consistent with the heart weight data shown in Fig. 2. Isolectin staining revealed that expression of Q510E-SHP2 in hearts with normal levels of AKT1 reduced the number of capillaries per area (Fig. 5C). Importantly, capillary density per area was increased back to control levels by concomitant deletion of one AKT1 allele (Fig. 5C). As shown in Fig. 5D, the resulting capillary-to-cardiomyocyte ratio was significantly increased in hearts from +;WT/− mice compared to the +;WT/WT and NTG;WT/− groups. Representative images of WGA and isolectin stainings are shown in Fig. 5E.

4. Discussion

In summary, this study shows that heterozygous deletion of AKT1 prevents the functional decline caused by cardiac-specific expression of Q510E-SHP2 in a transgenic mouse model of NSML-associated HCM. However, deletion of one AKT1 allele did not ameliorate cardiac hypertrophy despite normalization of pro-hypertrophic signaling at the level of ribosomal protein S6. Notably, the rescue in contractile function was associated with an increase in the capillary-to-cardiomyocyte ratio in ventricular tissue sections. Taken together, these findings indicate that AKT1 protein levels influence contractile dysfunction in Q510E-SHP2-associated HCM. In contrast, the data also demonstrate that AKT1 is unlikely to be the predominant driver of cardiomyocyte hypertrophy. Indirectly, our findings suggest that improved oxygen supply to the hypertrophied cardiomyocytes may be key to understanding the beneficial effects of AKT1 protein reduction.

In the light of our previous studies showing that rapamycin reduces cardiomyocyte hypertrophy both in vitro and in vivo [11,13], these findings were surprising. At first sight, one could surmise that mTOR and AKT1 might play distinct roles with respect to cardiac morphology and function. However, such a view would be incompatible with the literature. For example, there is strong evidence that AKT is required for normal organ growth [24,27]. Vice versa, mTOR has been shown to be involved in the regulation of cardiac function whilst not being essential for hypertrophic growth [28]. Therefore, our findings cannot be easily explained by pathway dichotomy and highlight that the interactions of AKT and mTOR are complex and context-dependent.

One possibility why the reduction in AKT1 protein levels may have failed to prevent hypertrophy is that targeting only one AKT isoform was insufficient. Cardiomyocytes contain AKT1, AKT2, and AKT3, with the latter being the least abundant isoform [17]. These three isoforms have distinct as well as partially overlapping functions, with AKT3 primarily promoting brain growth [29,30], AKT2 regulating cellular metabolism and survival [31–33], and AKT1 governing physiologic organ growth [23,24,27,34,35]. To some extent, compensation between the three isoforms is possible. For example, it has been reported that overexpression of AKT3 led to parallel downregulation of AKT1 and AKT2 [36]. In contrast, deletion of AKT2 did not affect protein levels of AKT1 and AKT3 [31], suggesting that compensatory mechanisms may not be present under all conditions. To take potential compensation into account, we examined phosphorylation levels of ribosomal protein S6, which as a downstream regulator of cell size reflects the summation of signals mediated by all three AKT isoforms. Notably, we found that phosphorylation of S6 in +;WT/− mice was significantly lower than in +;WT/WT mice, and appeared to be even slightly below the level

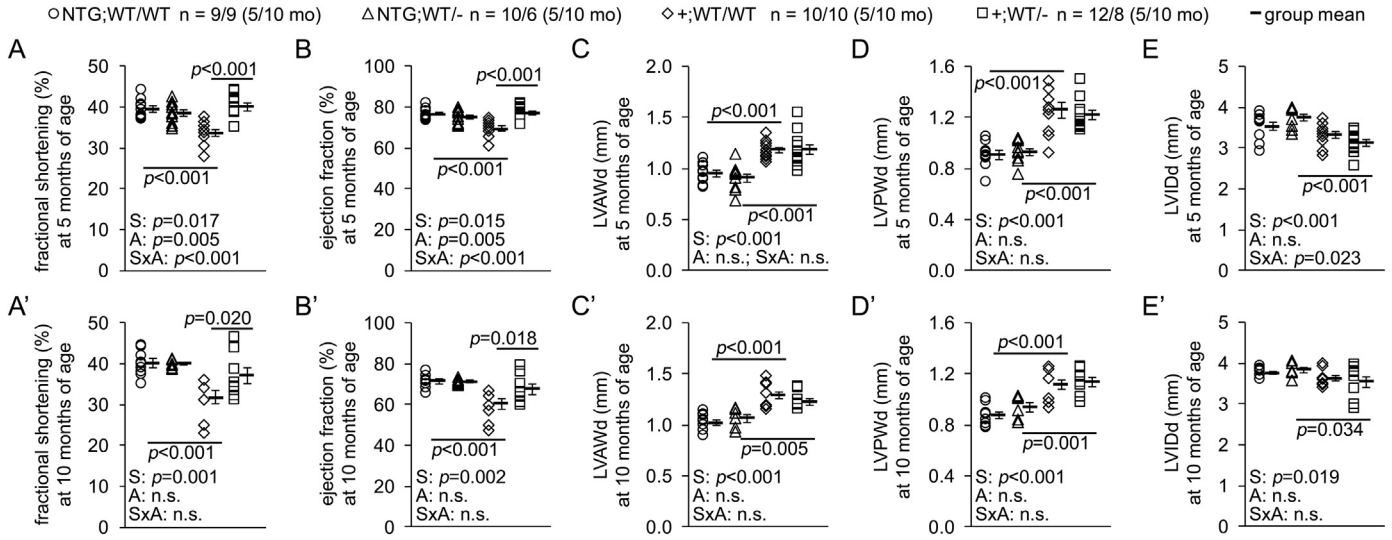

Fig. 4. Echocardiographic measurements. In all panels, individual data and group means +/− SEM are shown. Sample sizes for all groups are listed at the top. For all variables, graphs in the top row summarize data from 5 month-old mice, and graphs in the bottom row from 10 month-old mice. S, genotype regarding presence or absence of the Q510E-SHP2 transgene; A, genotype regarding presence of one or two AKT1 alleles; S × A, interaction between S and A. A,A′) LV fractional shortening was decreased by Q510E-SHP2 expression in mice with normal levels of AKT1. This effect was reversed by heterozygous AKT1 deletion. B,B′) LV ejection fraction was decreased by Q510E-SHP2 expression in mice with normal levels of AKT1. This effect was reversed by heterozygous AKT1 deletion. C,C′) LV anterior wall thickness at end-diastole (LVAWd) was increased by Q510E-SHP2 expression in mice with normal levels of AKT1. This was not rescued by heterozygous AKT1 deletion. D,D′) LV posterior wall thickness at end-diastole (LVPWd) was increased by Q510E-SHP2 expression in mice with normal levels of AKT1. This was not rescued by heterozygous AKT1 deletion. E,E′) LV inner diameter at end-diastole (LVIDd) was reduced by Q510E-SHP2 expression in mice missing one AKT1 allele.

observed in the NTG;WT/WT control group. Although there may have been some redundancy in function of the different AKT isoforms, this was not sufficient to sustain hyperactivation of S6. Consequently, it appears unlikely that our strategy of targeting only AKT1 failed due to compensatory hyperactivation of AKT2 and /or AKT3.

Alternatively, we could speculate that deletion of only one AKT1 allele was too mild to suppress the hypertrophic phenotype. Previously, in vitro studies in neonatal cardiomyocytes with adenovirus-mediated overexpression of Q510E-SHP2 demonstrated that AKT inhibitor VIII normalized cardiomyocyte sizes in culture at 2 and 4 μM concentration [11]. AKT inhibitor VIII has an IC50 of 58 nM for AKT1 [37], therefore AKT1 was most likely completely inhibited at the concentrations used. This could suggest that in the current study, heterozygous AKT1 deletion was insufficient to normalize signaling. Again, our S6 data speak against this interpretation, but S6 may not be the only critical downstream mediator. Since AKT signaling is essential for normal growth, complete inhibition of this pathway during prenatal development could be problematic as a therapeutic strategy. This is underlined by our finding that the combination of complete AKT1 deletion with Q510E-SHP2 expression severely reduced survival of +;−/− pups. At this point, we cannot exclude that for example a 75% reduction in AKT1 levels could have been effective to reduce cardiac hypertrophy as well as improve contractile function in mice. However, we would expect that a pharmacological intervention to achieve that precise level of suppression would be extremely challenging to titrate in the clinic.

Surprisingly, the extent of AKT1 and S6 hyperphosphorylation in response to Q510E-SHP2 expression was more subtle than we had previously observed in the FVB/N strain background [13]. We suspect that breeding over > 14 generations or strain background effects could have been responsible for these diminished signals. Importantly, there was no phenotype drift in our model after crossing from FVB/N into the C57BL/6J background. This supports that the relatively small increase in pathway activation seen in +;WT/WT compared to NTG;WT/WT heart tissue is still sufficient to induce the HCM phenotype.

However, recent studies have shown that a mild increase in AKT activation by itself does not induce pathologic hypertrophy [18,19]. This suggests that the HCM phenotype in our NSML model may be driven not solely by AKT/mTOR, but that other dysregulated signaling pathways may also play a role. For example, we previously noted that the level of ERK1/2 phosphorylation is also increased in Q510E-SHP2-expressing hearts [13], which may contribute to the phenotype. As many of SHP2's substrates have still not been clearly identified, the interactions of various SHP2-dependent pathways cannot be easily unraveled.

Furthermore, the timing of AKT hyperactivation could be the critical factor rather than the degree of hyperactivation. Interestingly, our previous data demonstrated that mice do not develop HCM if Q510E-SHP2 expression starts after birth driven by the α-MHC promoter [13]. Only if Q510E-SHP2 is already present during the prenatal time window, cardiac pathology is induced. This indicates that there is a vulnerable interval during which Q510E-SHP2 expression (and thereby downstream AKT hyperactivation) results in the development of HCM. Therefore, Q510E-SHP2 may disrupt critical steps in cardiac development thus laying the foundation for the development of HCM. Since myogenic AKT can regulate vascular growth [38], we examined the capillary network and in particular capillary-to-cardiomyocyte ratios more closely. Strikingly, Q510E-SHP2 expression reduced the number of capillaries per area, and combination with heterozygous AKT1 deletion reversed this effect. As a result, the ratio of capillaries to cardiomyocytes was highest in +;WT/− hearts. While the current data do not establish causality, one could speculate that perfusion and oxygen supply were improved in +;WT/− compared to +;WT/WT hearts, which could provide a reasonable explanation for the observed rescue in contractile performance.

Importantly, other mouse models support that the density of the capillary network is regulated by AKT and closely linked to pathologic alterations as well as cardioprotective effects. Deletion of PHLPP1 resulted in an increase in capillary density [19], whereas prolonged hyperactivation of AKT reduced the number of capillaries per area by impairing angiogenesis [39]. Studies in the retinal vasculature have shown that sustained AKT hyperactivation also disrupts vascular remodeling during development [40], indicating that AKT fine-tunes survival signaling to support appropriate vessel regression. Interestingly, too little AKT activity can also have detrimental effects. Complete deletion of AKT1 significantly reduced the number of capillaries per area in the myocardium [41]. Notably, deletion of only one AKT1 allele

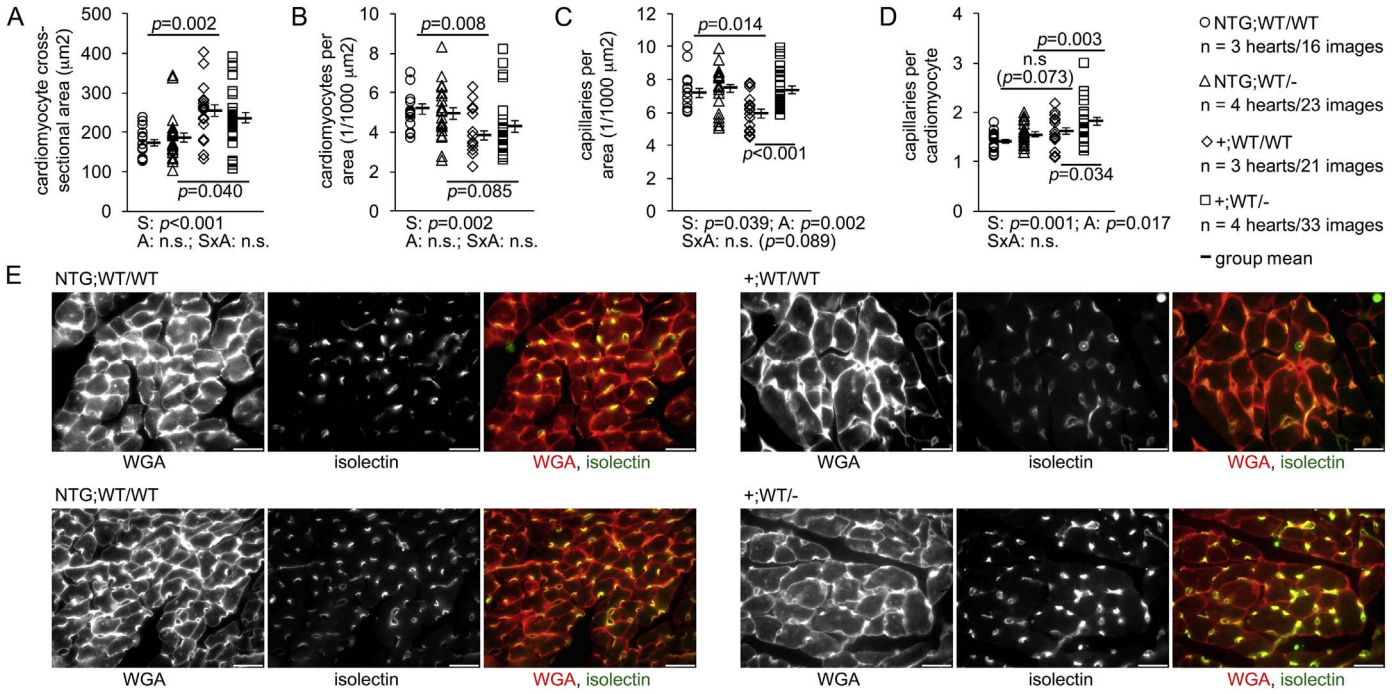

Fig. 5. Cardiomyocyte sizes and capillary density. In all panels, individual data and group means +/− SEM are shown. Sample sizes for all groups are listed at the top. All data were obtained in sections from 10-month old hearts stained with WGA to outline sarcolemma and isolectin to visualize capillaries. S, genotype regarding presence or absence of the Q510E-SHP2 transgene; A, genotype regarding presence of one or two AKT1 alleles; S × A, interaction between S and A. A) Cardiomyocyte cross-sectional area was increased by Q510E-SHP2 expression regardless of the level of AKT1 expression. B) Cardiomyocyte number per area was reduced by Q510E-SHP2 expression regardless of the level of AKT1 expression. C) Capillary number per area was reduced by Q510E-SHP2 expression in mice with normal AKT1 expression. This effect was reversed by additional heterozygous AKT1 deletion. D) The ratio of the number of capillaries per cardiomyocyte was increased by Q510E-SHP2 expression combined with heterozygous AKT1 deletion. E) Representative images of WGA- and isolectin-stained sections demonstrating increased cardiomyocyte sizes in Q510E-SHP2-expressing hearts, capillary rarefaction due to Q510E-SHP2 expression, and increased capillary-to-cardiomyocyte ratio in hypertrophied hearts with reduced AKT1 protein. All scale bars, 20 µm.

did not affect capillary density [41], as we also confirmed in the current study. Taken together, these studies indicate that appropriate AKT activation is critical for cardiac development and homeostasis, with too low as well as too high levels having deleterious effects.

In our NSML model, capillary rarefaction induced by Q510E-SHP2 expression was rescued by normalizing signaling through AKT1. Since this was directly associated with improved contractile performance, we speculate that therapeutic interventions to increase myocardial perfusion may improve clinical outcomes in this particular patient population. Our data do not allow extrapolation to other forms of HCM at this point, but coronary microvascular dysfunction is most likely responsible for the ischemia-like clinical signs and symptoms observed in more common forms of pathologic LV hypertrophy [42]. Furthermore, the degree of microvascular dysfunction is a strong and independent predictor of clinical deterioration and death in patients with HCM [43]. Therefore, the current findings may have important clinical implications for patients carrying the Q510E-SHP2 mutation and support a personalized medicine approach for NSML-associated HCM. In particular, our mouse model suggests that targeting AKT1 may improve coronary microcirculation and thereby possibly morbidity and mortality in NSML cases with impaired contractile performance of the hypertrophied ventricle.

5. Conclusions

This study demonstrates that normal levels of AKT1 are not required for cardiomyocyte hypertrophy induced by Q510E-SHP2 expression. However, a reduction in AKT1 protein rescued the functional decline in this particular form of HCM. As this rescue was associated with normalized capillary-to-cardiomyocyte ratios, targeting AKT1 could become a future therapeutic approach to improve coronary microcirculation and thereby myocardial oxygen supply. This has the potential to significantly improve morbidity and mortality in the clinic.

Disclosures/conflict of interest

None declared.

Acknowledgements and sources of funding

We thank Kathryn Crombie, Diana Douglas, and Jixia (Jessica) Meininger for their expert technical support. Research reported in this article was supported by the National Heart, Lung, and Blood Institute of the National Institutes of Health under award number R01HL116525 (to MK). The content is solely the responsibility of the authors and does not necessarily represent the official views of the National Institutes of Health.

References

[1] K.M. Harris, P. Spirito, M.S. Maron, A.G. Zenovich, F. Formisano, J.R. Lesser, S. Mackey-Bojack, W.J. Manning, J.E. Udelson, B.J. Maron, Prevalence, clinical profile, and significance of left ventricular remodeling in the end-stage phase of hypertrophic cardiomyopathy, Circulation 114 (3) (2006) 216–225.
[2] H. Morita, J. Seidman, C.E. Seidman, Genetic causes of human heart failure, J. Clin. Invest. 115 (3) (2005) 518–526.
[3] B.J. Maron, S.R. Ommen, C. Semsarian, P. Spirito, I. Olivotto, M.S. Maron, Hypertrophic cardiomyopathy: present and future, with translation into contemporary cardiovascular medicine, J. Am. Coll. Cardiol. 64 (1) (2014) 83–99.
[4] M.C. Digilio, A. Sarkozy, G. Pacileo, G. Limongelli, B. Marino, B. Dallapiccola, PTPN11 gene mutations: linking the Gln510Glu mutation to the "LEOPARD syndrome phenotype", Eur. J. Pediatr. 165 (11) (2006) 803–805.
[5] M.F. Faienza, L. Giordani, M. Ferraris, G. Bona, L. Cavallo, PTPN11 gene mutation and severe neonatal hypertrophic cardiomyopathy: what is the link? Pediatr. Cardiol. 30 (7) (2009) 1012–1015.

[6] M. Ganigara, A. Prabhu, R.S. Kumar, LEOPARD syndrome in an infant with severe hypertrophic cardiomyopathy and PTPN11 mutation, Ann. Pediatr. Cardiol. 4 (1) (2011) 74–76.
[7] K. Takahashi, S. Kogaki, S. Kurotobi, S. Nasuno, M. Ohta, H. Okabe, K. Wada, N. Sakai, M. Taniike, K. Ozono, A novel mutation in the PTPN11 gene in a patient with Noonan syndrome and rapidly progressive hypertrophic cardiomyopathy, Eur. J. Pediatr. 164 (8) (2005) 497–500.
[8] T. Konno, S. Chang, J.G. Seidman, C.E. Seidman, Genetics of hypertrophic cardiomyopathy, Curr. Opin. Cardiol. 25 (3) (2010) 205–209.
[9] T. Edouard, J.P. Combier, A. Nedelec, S. Bel-Vialar, M. Metrich, F. Conte-Auriol, S. Lyonnet, B. Parfait, M. Tauber, J.P. Salles, F. Lezoualc'h, A. Yart, P. Raynal, Functional effects of PTPN11 (SHP2) mutations causing LEOPARD syndrome on epidermal growth factor-induced phosphoinositide 3-kinase/AKT/glycogen synthase kinase 3beta signaling, Mol. Cell. Biol. 30 (10) (2010) 2498–2507.
[10] H. Ishida, S. Kogaki, J. Narita, H. Ichimori, N. Nawa, Y. Okada, K. Takahashi, K. Ozono, LEOPARD-type SHP2 mutant Gln510Glu attenuates cardiomyocyte differentiation and promotes cardiac hypertrophy via dysregulation of Akt/GSK-3{beta}/{beta}-catenin signaling, Am. J. Physiol. Heart Circ. Physiol. 301 (4) (2011) H1531–9.
[11] C. Schramm, M.A. Edwards, M. Krenz, New approaches to prevent LEOPARD syndrome-associated cardiac hypertrophy by specifically targeting Shp2-dependent signaling, J. Biol. Chem. 288 (25) (2013) 18335–18344.
[12] T.M. Marin, K. Keith, B. Davies, D.A. Conner, P. Guha, D. Kalaitzidis, X. Wu, J. Lauriol, B. Wang, M. Bauer, R. Bronson, K.G. Franchini, B.G. Neel, M.I. Kontaridis, Rapamycin reverses hypertrophic cardiomyopathy in a mouse model of LEOPARD syndrome-associated PTPN11 mutation, J. Clin. Invest. 121 (3) (2011) 1026–1043.
[13] C. Schramm, D.M. Fine, M.A. Edwards, A.N. Reeb, M. Krenz, The PTPN11 loss-of-function mutation Q510E-Shp2 causes hypertrophic cardiomyopathy by dysregulating mTOR signaling, Am. J. Physiol. Heart Circ. Physiol. 302 (1) (2012) H231–43.
[14] C.J. Potter, L.G. Pedraza, T. Xu, Akt regulates growth by directly phosphorylating Tsc2, Nat. Cell Biol. 4 (9) (2002) 658–665.
[15] K. Inoki, Y. Li, T. Zhu, J. Wu, K.L. Guan, TSC2 is phosphorylated and inhibited by Akt and suppresses mTOR signalling, Nat. Cell Biol. 4 (9) (2002) 648–657.
[16] E. Rozengurt, H.P. Soares, J. Sinnet-Smith, Suppression of feedback loops mediated by PI3K/mTOR induces multiple overactivation of compensatory pathways: an unintended consequence leading to drug resistance, Mol. Cancer Ther. 13 (11) (2014) 2477–2488.
[17] M.A. Sussman, M. Volkers, K. Fischer, B. Bailey, C.T. Cottage, S. Din, N. Gude, D. Avitabile, R. Alvarez, B. Sundararaman, P. Quijada, M. Mason, M.H. Konstandin, A. Malhowski, Z. Cheng, M. Khan, M. McGregor, Myocardial AKT: the omnipresent nexus, Physiol. Rev. 91 (3) (2011) 1023–1070.
[18] O.J. Kemi, M. Ceci, U. Wisloff, S. Grimaldi, P. Gallo, G.L. Smith, G. Condorelli, O. Ellingsen, Activation or inactivation of cardiac Akt/mTOR signaling diverges physiological from pathological hypertrophy, J. Cell. Physiol. 214 (2) (2008) 316–321.
[19] C. Moc, A.E. Taylor, G.P. Chesini, C.M. Zambrano, M.S. Barlow, X. Zhang, A.B. Gustafsson, N.H. Purcell, Physiological activation of Akt by PHLPP1 deletion protects against pathological hypertrophy, Cardiovasc. Res. 105 (2) (2015) 160–170.
[20] M. Rota, A. Boni, K. Urbanek, M.E. Padin-Iruegas, T.J. Kajstura, G. Fiore, H. Kubo, E.H. Sonnenblick, E. Musso, S.R. Houser, A. Leri, M.A. Sussman, P. Anversa, Nuclear targeting of Akt enhances ventricular function and myocyte contractility, Circ. Res. 97 (12) (2005) 1332–1341.
[21] Y. Tsujita, J. Muraski, I. Shiraishi, T. Kato, J. Kajstura, P. Anversa, M.A. Sussman, Nuclear targeting of Akt antagonizes aspects of cardiomyocyte hypertrophy, Proc. Natl. Acad. Sci. U. S. A. 103 (32) (2006) 11946–11951.
[22] T. Matsui, L. Li, J.C. Wu, S.A. Cook, T. Nagoshi, M.H. Picard, R. Liao, A. Rosenzweig, Phenotypic spectrum caused by transgenic overexpression of activated Akt in the heart, J. Biol. Chem. 277 (25) (2002) 22896–22901.
[23] H. Cho, J.L. Thorvaldsen, Q. Chu, F. Feng, M.J. Birnbaum, Akt1/PKBalpha is required for normal growth but dispensable for maintenance of glucose homeostasis in mice, J. Biol. Chem. 276 (42) (2001) 38349–38352.
[24] B. DeBosch, I. Treskov, T.S. Lupu, C. Weinheimer, A. Kovacs, M. Courtois, A.J. Muslin, Akt1 is required for physiological cardiac growth, Circulation 113 (17) (2006) 2097–2104.
[25] S.A. Clay, T.L. Domeier, L.M. Hanft, K.S. McDonald, M. Krenz, Elevated Ca2 + transients and increased myofibrillar power generation cause cardiac hypercontractility in a model of Noonan syndrome with Multiple Lentigines, Am. J. Physiol. Heart Circ. Physiol. 308 (9) (2015) H1086–95.
[26] T. Nakamura, M. Colbert, M. Krenz, J.D. Molkentin, H.S. Hahn, G.W. Dorn, J. Robbins 2nd, Mediating ERK 1/2 signaling rescues congenital heart defects in a mouse model of Noonan syndrome, J. Clin. Invest. 117 (8) (2007) 2123–2132.
[27] T. Shioi, J.R. McMullen, P.M. Kang, P.S. Douglas, T. Obata, T.F. Franke, L.C. Cantley, S. Izumo, Akt/protein kinase B promotes organ growth in transgenic mice, Mol. Cell. Biol. 22 (8) (2002) 2799–2809.
[28] W.H. Shen, Z. Chen, S. Shi, H. Chen, W. Zhu, A. Penner, G. Bu, W. Li, D.W. Boyle, M. Rubart, L.J. Field, R. Abraham, E.A. Liechty, W. Shou, Cardiac restricted overexpression of kinase-dead mammalian target of rapamycin (mTOR) mutant impairs the mTOR-mediated signaling and cardiac function, J. Biol. Chem. 283 (20) (2008) 13842–13849.
[29] O. Tschopp, Z.Z. Yang, D. Brodbeck, B.A. Dummler, M. Hemmings-Mieszczak, T. Watanabe, T. Michaelis, J. Frahm, B.A. Hemmings, Essential role of protein kinase B gamma (PKB gamma/Akt3) in postnatal brain development but not in glucose homeostasis, Development 132 (13) (2005) 2943–2954.
[30] R.M. Easton, H. Cho, K. Roovers, D.W. Shineman, M. Mizrahi, M.S. Forman, V.M. Lee, M. Szabolcs, R. de Jong, T. Oltersdorf, T. Ludwig, A. Efstratiadis, M.J. Birnbaum, Role for Akt3/protein kinase Bgamma in attainment of normal brain size, Mol. Cell. Biol. 25 (5) (2005) 1869–1878.
[31] H. Cho, J. Mu, J.K. Kim, J.L. Thorvaldsen, Q. Chu, E.B. Crenshaw 3rd, K.H. Kaestner, M.S. Bartolomei, G.I. Shulman, M.J. Birnbaum, Insulin resistance and a diabetes mellitus-like syndrome in mice lacking the protein kinase Akt2 (PKB beta), Science 292 (5522) (2001) 1728–1731.
[32] B. DeBosch, N. Sambandam, C. Weinheimer, M. Courtois, A.J. Muslin, Akt2 regulates cardiac metabolism and cardiomyocyte survival, J. Biol. Chem. 281 (43) (2006) 32841–32851.
[33] A.J. Muslin, Akt2: a critical regulator of cardiomyocyte survival and metabolism, Pediatr. Cardiol. 32 (3) (2011) 317–322.
[34] W.S. Chen, P.Z. Xu, K. Gottlob, M.L. Chen, K. Sokol, T. Shiyanova, I. Roninson, W. Weng, R. Suzuki, K. Tobe, T. Kadowaki, N. Hay, Growth retardation and increased apoptosis in mice with homozygous disruption of the Akt1 gene, Genes Dev. 15 (17) (2001) 2203–2208.
[35] G. Condorelli, A. Drusco, G. Stassi, A. Bellacosa, R. Roncarati, G. Iaccarino, M.A. Russo, Y. Gu, N. Dalton, C. Chung, M.V. Latronico, C. Napoli, J. Sadoshima, C.M. Croce, J. Ross Jr., Akt induces enhanced myocardial contractility and cell size in vivo in transgenic mice, Proc. Natl. Acad. Sci. U. S. A. 99 (19) (2002) 12333–12338.
[36] Y. Taniyama, M. Ito, K. Sato, C. Kuester, K. Veit, G. Tremp, R. Liao, W.S. Colucci, Y. Ivashchenko, K. Walsh, I. Shiojima, Akt3 overexpression in the heart results in progression from adaptive to maladaptive hypertrophy, J. Mol. Cell. Cardiol. 38 (2) (2005) 375–385.
[37] C.W. Lindsley, Z. Zhao, W.H. Leister, R.G. Robinson, S.F. Barnett, D. Defeo-Jones, R.E. Jones, G.D. Hartman, J.R. Huff, H.E. Huber, M.E. Duggan, Allosteric Akt (PKB) inhibitors: discovery and SAR of isozyme selective inhibitors, Bioorg. Med. Chem. Lett. 15 (3) (2005) 761–764.
[38] A. Takahashi, Y. Kureishi, J. Yang, Z. Luo, K. Guo, D. Mukhopadhyay, Y. Ivashchenko, D. Branellec, K. Walsh, Myogenic Akt signaling regulates blood vessel recruitment during myofiber growth, Mol. Cell. Biol. 22 (13) (2002) 4803–4814.
[39] I. Shiojima, K. Sato, Y. Izumiya, S. Schiekofer, M. Ito, R. Liao, W.S. Colucci, K. Walsh, Disruption of coordinated cardiac hypertrophy and angiogenesis contributes to the transition to heart failure, J. Clin. Invest. 115 (8) (2005) 2108–2118.
[40] J.F. Sun, T. Phung, I. Shiojima, T. Felske, J.N. Upalakalin, D. Feng, T. Kornaga, T. Dor, A.M. Dvorak, K. Walsh, L.E. Benjamin, Microvascular patterning is controlled by fine-tuning the Akt signal, Proc. Natl. Acad. Sci. U. S. A. 102 (1) (2005) 128–133.
[41] K. Vandoorne, M.H. Vandsburger, K. Weisinger, V. Brumfeld, B.A. Hemmings, A. Harmelin, M. Neeman, Multimodal imaging reveals a role for Akt1 in fetal cardiac development, Phys. Rep. 1 (6) (2013) e00143.
[42] P.G. Camici, I. Olivotto, O.E. Rimoldi, The coronary circulation and blood flow in left ventricular hypertrophy, J. Mol. Cell. Cardiol. 52 (4) (2012) 857–864.
[43] F. Cecchi, I. Olivotto, R. Gistri, R. Lorenzoni, G. Chiriatti, P.G. Camici, Coronary microvascular dysfunction and prognosis in hypertrophic cardiomyopathy, N. Engl. J. Med. 349 (11) (2003) 1027–1035.